Bird Protection Zones in a Wind Park by Ka-Band Radar Surveillance: Field Results from the Wind Testing Site WINSENT

Moritz Mälzer[*], Marcel Burhenn[†], Sebastian Beck[*], Ashkan Taremi Zadeh[*], Jochen Moll[*], Viktor Krozer[*], Daniel Hübsch[†], Andreas Nuber[‡], Michael Werner[§], Stefan Kaminsky[§]

[*]Goethe University of Frankfurt, Department of Physics, 60438 Frankfurt am Main, Germany,
E-Mail: moll@physik.uni-frankfurt.de
[†]HÜBNER GmbH & Co. KG, 34123 Kassel, Germany
[‡]Wölfel Engineering GmbH + Co. KG, Höchberg, Germany
[§]Kaminsky Naturschutzplanung GmbH, 97618 Hohenroth, Germany

***Abstract*—In this paper, we report on a newly developed 34 GHz radar system and its field application in the wind energy testing site WINSENT on the Swabian Alb (Germany). The envisaged sensor system addresses the early detection of birds for a bird-friendly wind turbine operation. In this way, wind turbines could be adaptively controlled to reduce the collision risk of endangered species. Besides the description of the radar sensor and its characterization in the laboratory, we also demonstrate the system implementation using three Ka-band radar units. Bird detection results are presented along with a synchronized camera-based validation.**

***Index Terms*—Wind turbines, detection of birds, monitoring, radar systems**

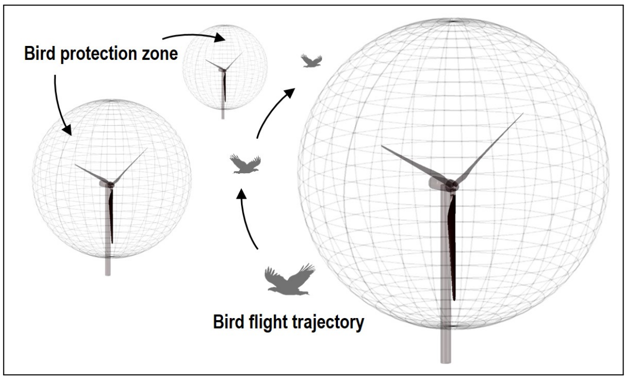

Fig. 1. Bird protection zones in a wind park by radar surveillance

I. Introduction

In order to achieve the goals of the Paris climate agreement, a massive increase in renewable energies is required. In the RESCUE study of the German Federal Environment Agency (*Umweltbundesamt*) various scenarios are considered towards resource-conserving greenhouse gas neutrality [1]. In each scenario, onshore wind energy plays the largest role in energy generation with up to 57 % in 2050. This means, that the green-green dilemma considering wind energy on one hand and the conservation of biodiversity on the other hand is a challenge for today and also in the future [2].

It is well known that bats and birds are affected by the collision with the rotor blades and that bats can also die from barotrauma [3], [4]. In order to reduce bird and bat mortality different mitigation strategies are possible. This paper will focus on the conservation of birds by means of a sensorized anti-collision system.

Besides fixed shutdown times, e.g. during the breeding season, an adaptive wind turbine control is a possible solution. This means that wind turbines are only switched off in the presence of relevant animal species. This approach could open up new locations for wind turbines that would otherwise not be approvable or economically viable. For example, shutdown times could be reduced to a minimum to maximize energy production. Event-based shutdowns, e.g. after mowing, could be automated as well.

Currently, several systems are being developed or already employed aiming at bird-friendly wind turbine operation [5]. Examples include the *SafeWind* system [6] where cameras are mounted on the wind turbine tower reaching detection distances of about 300 m to 600 m depending on the species. On the other hand, the camera-based system *IdentiFlight* [7] reaches distances of about 1 km.

Radar systems, on the other hand, have the advantage to support day and night operation as well as their usage in the rain and in the fog. There are several radar-based systems available. Most of these radar systems operate in X-band between 8 GHz and 12 GHz. The detection range of these systems is 1 km to 7 km depending on the species. Some radar systems, such as *RobinRadar MAX* [8], operate with rotating antennas. The *BirdScan MS1* [9] radar, on the other hand, uses a fixed radar beam. Both systems have in common that they are free-standing, and are thus particularly suitable for monitoring larger areas, such as entire wind farms. Radar systems at higher frequencies could be used for bird monitoring as well [10].

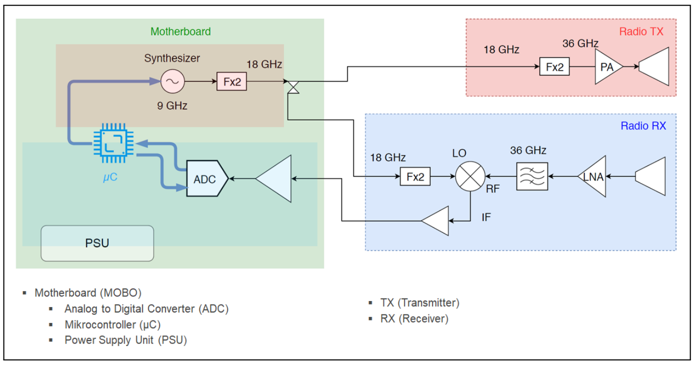

Fig. 2. Simplified block diagram of the Ka-band radar.

The idea of the current work is to completely cover the near field of a single wind turbine with several Ka-band radar sensors with a fixed radar beam around the wind turbine tower as shown in Fig. 1, see also [11]. This approach could be more cost-effective compared to the previously mentioned camera-based and X-band radar solution. In the present study, the concept will be demonstrated by an implementation of three radar systems at the wind energy test field *WINSENT* on the Swabian Alb (Germany) during the period from June to October 2021.

II. Description of the FMCW Radar Sensor

A novel frequency-modulated continuous wave (FMCW) radar sensor has been developed in this work operating from 33.4 to 34.15 GHz with a sweep time of 2.56 ms. Each sensor consists of three modular units, i.e. a transmitter frontend, a receiver frontend and a mainboard. A simplified block diagram of these units is depicted in Fig. 2. The mainboard has several tasks: It provides the DC power supply preregulated by a bunch of wide range switching regulators, generates the local oscillator (LO) signal for the frontend modules and processes the intermediate frequency (IF). The IF signal undergoes some amplification stages and finally gets A/D converted. The digital signal is processed by a microcontroller and sent over Ethernet to the measurement computer. Fig. 3 shows a photo of the radar sensor.

One key aspect for the field study is the stability of the receiver and transmitter front end. Time domain stability was tested prior to the field studies for both entities. As depicted in Fig. 4 a vector network analyzer (VNA) is used to drive the LO input of the transmitter frontend as well as the LO input of a separate frequency doubler which provides LO input for a mixer. The mixer is used as a down converter and due to the high output power level of the transmitter front end (TX) a reasonable attenuation is inserted to protect the mixer. A spectrum analyzer is used to measure the down converted signal level. This setup was used with remote control of a computer collecting a proportional value to the output power of the transmitter. Results for the transmitter and for the receiver are depicted in Fig. 5 and Fig. 6, respectively. The setup for the IF deviation measurement is different from the transmitter measurement setup but the results are similar.

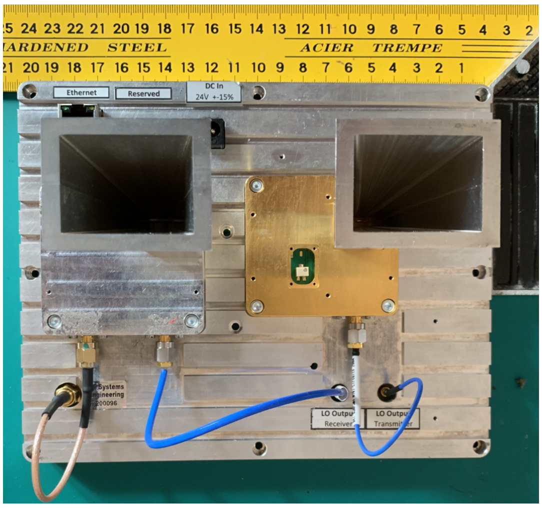

Fig. 3. Photo of the Ka-band radar with two horn antennas.

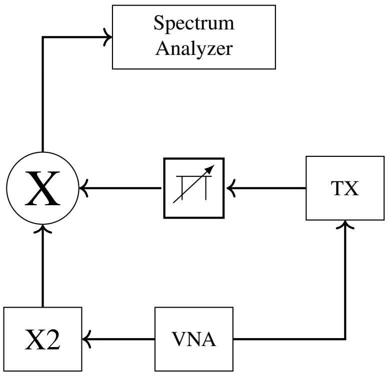

Fig. 4. Measurement setup for time domain stability evaluation of the transmitter front end (TX)

The measured output power at the transmitter was 27.8 dBm prior to the field studies. After the field studies the output power of this system was measured again and the output power was in the same range, i.e. 28.9 dBm.

III. Description of the Field Study Design

A. Hardware

The field study has been implemented at the wind energy testing site WINSENT. Figs. 7 and 8 show the measurement system mounted on the wind measuring mast. It consisted of three modules, each equipped with a radar sensor, a 180-degree-camera and an ultrasonic microphone. The ultrasonic microphones were integrated in the radar housing.

The modules were mounted so that each module covers one side of the wind measuring mast. With the three 180-degree-camera we achieved a full 360 degree coverage. They mainly served as visual verification for the radar measurements. The radars had horn antennas with a gain of up to 17 dBi, i.e. approximately 20°. This naturally results in a smaller aperture angle than the cameras.

All modules were connected to a control cabinet that consists of the power supply, a computer for controlling the

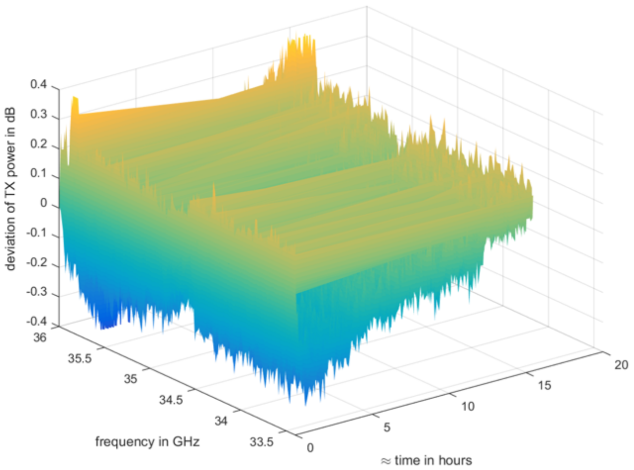

Fig. 5. TX power deviation of one TX front end module over time.

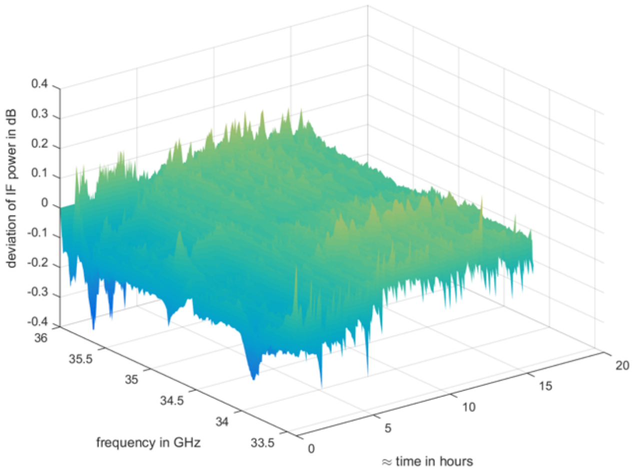

Fig. 6. IF power deviation of one RX front end module over time.

measurements and an LTE modem for remote maintenance and data transmission.

B. Software

The software on the measurement computer analyzed the incoming data in real-time, triggered and collected the data from the different sensor sources in a synchronous and autonomous way. The camera triggered an event when an object moved inside the detection area. The radar triggered via a distance-dependent threshold crossing. The statistically defined threshold accounted dynamically to the current environmental conditions [12]. A static threshold was chosen for the microphone, which was tested against the amplitude of the FFT in the frequency range between 40 kHz and 130 kHz.

IV. Results

During the field study a total number of 68 bird events have been recorded. A subset of 47 was automatically triggered by the radar. The rest was triggered by the camera subsystem.

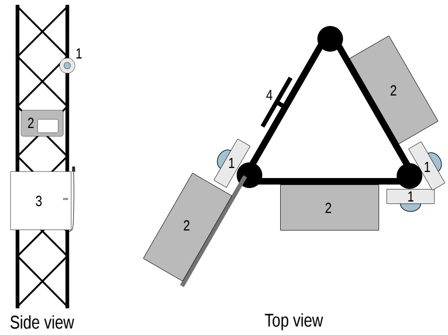

Fig. 7. Schematic view: 1. camera, 2. radar housing, 3. control cabinet, 4. ladder of the mast

Fig. 8. Photo of the field installation at WINSENT.

Below are some examples of recordings in which carrion crows were detected.

Figs. 9 and 10 show a photo and the corresponding radargram of a crow passing the radar system. In addition, Figs. 11 and 12 show a crow taking off from the mast above the radar and then moving radially away from the mast.

The radar system can detect birds up to about 35 m. This was verified by testing the system with a drone which has approximately the size of a medium sized bird (obviously with a different radar cross-section). Also, the birds are only visible for a few seconds in the radargram. This can be explained by the relatively strong focusing of the radar beam.

V. Conclusions

In this paper, it was shown that a system consisting of three Ka-band radar systems could be used to detect birds during a field study at the wind test site WINSENT. About 68 bird events have been recorded from which most have been automatically triggered by the radar subsystem.

However, on the radar side there is still potential for further developments. The current detection range of approx. 35 m is not sufficient to stop a wind turbine in time. For example, a red kite would have to be detected at a distance of at least 400 meters. To achieve this, the radar performance must be significantly improved in future developments. Since a single radar system has an aperture angle of only about 20°, several

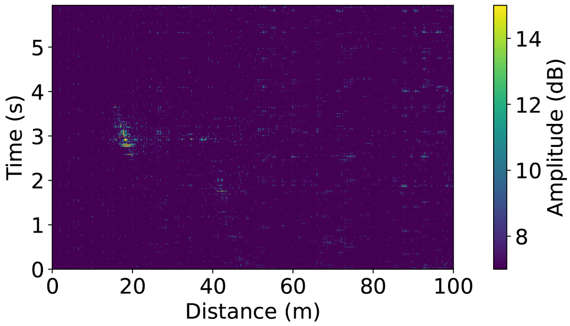

Fig. 9. Radargram of a carrion crow passing the radar.

Fig. 10. Image of the crow detected in the radargram in Fig. 9.

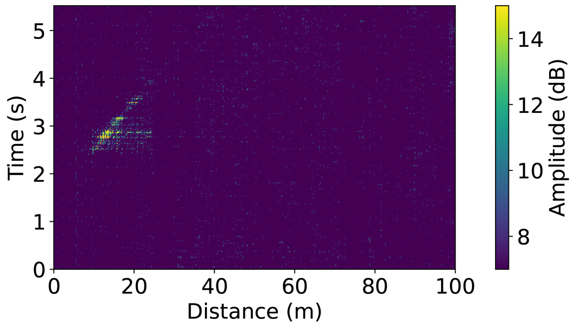

Fig. 11. Radargram of a carrion crow flying away from the radar.

Fig. 12. Image of the crow detected in the radargram in Fig. 11.

radar systems are needed for a complete coverage of the relevant airspace.

ACKNOWLEDGMENT

The authors gratefully acknowledge the financial support of this research by the Federal Ministry for Economic Affairs and Energy (grant number: 0324323C).

REFERENCES

[1] Katja Purr, Jens Günther, Harry Lehmann, and Philip Nuss, "Wege in eine ressourcenschonende Treibhausgasneutralität," Umweltbundesamt, Tech. Rep. 36/2019, Nov. 2019. [Online]. Available: https://www.umweltbundesamt.de/rescue

[2] T. M. Straka, M. Fritze, and C. C. Voigt, "The human dimensions of a green–green-dilemma: Lessons learned from the wind energy — wildlife conflict in Germany," *Energy Reports*, vol. 6, pp. 1768–1777, Nov. 2020. [Online]. Available: https://linkinghub.elsevier.com/retrieve/pii/S2352484720306466

[3] C. B. Thaxter, G. M. Buchanan, J. Carr, S. H. M. Butchart, T. Newbold, R. E. Green, J. A. Tobias, W. B. Foden, S. O'Brien, and J. W. Pearce-Higgins, "Bird and bat species' global vulnerability to collision mortality at wind farms revealed through a trait-based assessment," *Proceedings of the Royal Society B: Biological Sciences*, vol. 284, no. 1862, p. 20170829, Sep. 2017. [Online]. Available: https://royalsocietypublishing.org/doi/10.1098/rspb.2017.0829

[4] E. F. Baerwald, G. H. D'Amours, B. J. Klug, and R. M. Barclay, "Barotrauma is a significant cause of bat fatalities at wind turbines," *Current Biology*, vol. 18, no. 16, pp. R695–R696, Aug. 2008. [Online]. Available: https://linkinghub.elsevier.com/retrieve/pii/S0960982208007513

[5] K. Ammermann, E. Bruns, J. Ponitka, E. Schuster, D. Sudhaus, and F. Tucci, *Technische Systeme zur Minderung von Vogelkollisionen an Windenergieanlagen*, five hundred seventy-first ed. DE: Bundesamt für Naturschutz, 2020. [Online]. Available: https://doi.org/10.19217/skr571

[6] Joachim Steinmetz, "SafeWind – Der aktuelle Stand der Dinge," Linstow, Nov. 2018. [Online]. Available: https://windenergietage.de/2018/wp-content/uploads/sites/3/2018/11/27WT08_F14_1000_Fokus_Oekologie_SafeWind_.pdf

[7] C. J. McClure, L. Martinson, and T. D. Allison, "Automated monitoring for birds in flight: Proof of concept with eagles at a wind power facility," *Biological Conservation*, vol. 224, pp. 26–33, Aug. 2018. [Online]. Available: https://linkinghub.elsevier.com/retrieve/pii/S0006320717319407

[8] Hein Prinsen, "Using dedicated full 3D bird radar to assess bird flight behavior and collision risk at wind farms in the Netherlands," Nov. 2018. [Online]. Available: https://2018wwrm.exordo.com/programme/presentation/45

[9] Daniel Früh, "Raumüberwachung und Schutz von Grossvögeln mittels Radar," Kassel, 15.5.19. [Online]. Available: https://www.naturschutz-energiewende.de/wp-content/uploads/Frueh_KNE-Konferenz.pdf

[10] M. Mälzer, A. Taremi Zadeh, S. Beck, J. Moll, and V. Krozer, "Towards radar barriers for animal fatality detection at wind turbines: Numerical and preliminary experimental results," *IET Radar, Sonar & Navigation*, vol. 14, no. 11, pp. 1767–1772, Nov. 2020. [Online]. Available: https://onlinelibrary.wiley.com/doi/10.1049/iet-rsn.2020.0226

[11] A. T. Zadeh, M. Mälzer, D. H. Nguyen, J. Moll, and V. Krozer, "Radar-based Detection of Birds at Wind Turbines: Numerical Analysis for Optimum Coverage," in *2021 15th European Conference on Antennas and Propagation (EuCAP)*. Dusseldorf, Germany: IEEE, Mar. 2021, pp. 1–5. [Online]. Available: https://ieeexplore.ieee.org/document/9411349/

[12] J. Moll, J. Simon, M. Malzer, V. Krozer, D. Pozdniakov, R. Salman, M. Durr, M. Feulner, A. Nuber, and H. Friedmann, "Radar Imaging System for in-Service Wind Turbine Blades Inspections: Initial Results from a Field Installation at a 2 MW Wind Turbine," *Progress In Electromagnetics Research*, vol. 162, pp. 51–60, 2018. [Online]. Available: http://www.jpier.org/PIER/pier.php?paper=18021905